Published in final edited form as:
ACS Chem Biol. 2013 September 20; 8(9): 1998–2008. doi:10.1021/cb4003392.

Engineering unnatural variants of plantazolicin through codon reprogramming

Caitlin D. Deane[1,2], **Joel O. Melby**[1,2], **Katie J. Molohon**[2,3], **Aziz R. Susarrey**[4], and **Douglas A. Mitchell**[1,2,3,*]

[1]Department of Chemistry, University of Illinois at Urbana-Champaign, Urbana, Illinois, USA

[2]Institute for Genomic Biology, University of Illinois at Urbana-Champaign, Urbana, Illinois, USA

[3]Department of Microbiology, University of Illinois at Urbana-Champaign, Urbana, Illinois, USA

[4]School of Molecular and Cellular Biology, University of Illinois at Urbana-Champaign, Urbana, Illinois, USA

Abstract

Plantazolicin (PZN) is a polyheterocyclic natural product derived from a ribosomal peptide that harbors remarkable antibiotic selectivity for the causative agent of anthrax, *Bacillus anthracis*. To simultaneously establish the structure-activity relationship of PZN and the substrate tolerance of the biosynthetic pathway, an *Escherichia coli* expression strain was engineered to heterologously produce PZN analogs. Variant PZN precursor genes were produced by site-directed mutagenesis and later screened by mass spectrometry to assess posttranslational modification and export by *E. coli*. From a screen of 72 precursor peptides, 29 PZN variants were detected. This analog collection provided insight into the selectivity of the posttranslational modifying enzymes and established the boundaries of the natural biosynthetic pathway. Unlike other studied thiazole/oxazole-modified microcins, the biosynthetic machinery appeared to be finely tuned towards the production of PZN, such that the cognate enzymes did not process even other naturally occurring sequences from similar biosynthetic clusters. The modifying enzymes were exquisitely selective, installing heterocycles only at pre-defined positions within the precursor peptides while leaving neighboring residues unmodified. Nearly all substitutions at positions normally harboring heterocycles prevented maturation of a PZN variant, though some exceptions were successfully produced lacking a heterocycle at the penultimate residue. No variants containing additional heterocycles were detected, although several peptide sequences yielded multiple PZN variants as a result of varying oxidation states of select residues. Eleven PZN variants were produced in sufficient quantity to facilitate purification and assessment of their antibacterial activity, providing insight into the structure-activity relationship of PZN.

INTRODUCTION

The clinical deployment of antibiotics revolutionized medical practice in the 20th century, but beginning in the late 1960s, the development of new classes of antibiotics slowed drastically while bacteria continued to acquire resistance (1). Natural products have

*Corresponding author: Mitchell, Douglas (douglasm@illinois.edu), phone: 1-217-333-1345, fax: 1-217-333-0508.

The authors declare that they have no conflict of interest.

SUPPORTING INFORMATION

Supporting methods, design of mutant panels, purification and mass spectrometric analysis of PZN variants, sequences of chimera peptides, and DNA sequences can be found in the Supporting Information. This material is available free of charge *via* the Internet at http://pubs.acs.org.

historically been the most valuable source of antibiotics and still today present a promising avenue to combat the growing problem of infections caused by antibiotic-resistant bacteria. Indeed, of the new antibacterial compounds approved by the FDA between 1981 and 2010, 66% were natural products or natural product-derived (2). In recent years, the increased ease of bacterial genome sequencing has facilitated the development of new strategies to tap into unexplored regions of natural product chemical space (3). Natural product biosynthesis can potentially be "reprogrammed" to produce novel variants through genetic manipulation and/or supplying alternate substrates. Natural product engineering in modular biosynthetic pathways, such as polyketide synthases or non-ribosomal peptide synthetases, remains difficult due to the complex nature of the multi-domain megasynthases (4–7). In contrast, the reprogramming of ribosomally synthesized and post-translationally modified peptides (RiPPs) is straightforward, as the natural product structure is directly encoded by the sequence of the precursor peptide gene (8). Thus, site-directed mutagenesis leads to a predictable outcome in the resultant natural product, provided the modification enzymes tolerate the unnatural sequence.

Precursor peptide replacement *in vivo* has been used to study multiple RiPPs, most notably the lantibiotic nisin (9–11), leading to the identification of multiple variants with increased activity. Similar approaches have also been applied to the study of other lanthipeptides, including lacticin 3147 (12, 13), mersacidin (14), lichenicidin (15), and actagardine A (16). This strategy has also garnered recent attention outside of the lanthipeptide family, where it has been successfully employed to engineer novel variants and explore the substrate requirements for the precursor peptides of several thiopeptides (17–21), cyanobactins (22) and microcin J25 (23).

The thiazole/oxazole-modified microcins (TOMMs) (8) comprise one RiPP subfamily characterized by thiazoline, (methyl)oxazoline, and the corresponding 2-electron oxidized azoles, deriving from cysteines, serines, and threonines (Figure 1) (24). A trimeric enzymatic complex of a cyclodehydratase (C and D proteins) and a FMN-dependent dehydrogenase (B protein) catalyzes heterocycle formation and oxidation (Figure 1c) (24, 25). Plantazolicin (PZN), a TOMM produced by the soil bacterium, *Bacillus amyloliquefaciens* FZB42, displays a unique polyheterocyclic structure. After heterocycle formation, the unmodified *N*-terminal (leader peptide) region of the precursor peptide is proteolytically removed, likely by the putative peptidase (E protein) encoded in the gene cluster (Figure 1a) (26, 27). Lastly, two methyl groups are installed onto the new *N*-terminus of the core peptide by an *S*-adenosylmethionine (SAM)-dependent methyltransferase (L protein) to yield the mature natural product (Figure 1d), which is then predicted to be exported by a dedicated transporter (G and H proteins), also within in the gene cluster (26, 27).

PZN exhibits highly discriminating antibacterial activity against the causative agent of anthrax, *Bacillus anthracis* (27). The spectrum of PZN activity excludes all Gram-negative strains and most Gram-positive strains tested thus far. Exploration within the closely related *B. cereus* subgroup revealed *B. anthracis* as the only strain significantly susceptible to PZN (27). To date, similar biosynthetic gene clusters have been identified in four other bacterial species, indicating that these species have (or had at one time) the genetic capacity to produce PZN-like compounds, although only *B. pumilus* has been shown to do so during laboratory cultivation (27). The precursor peptides in these species display a high degree of sequence similarity to the PZN precursor peptide (BamA), including many conserved residues in the core peptide (Figure 1b) (27). However, the role that these conserved residues play in the posttranslational modification of PZN and their importance in the bioactivity of the mature compound remained unknown. The current study sought to simultaneously address the structure-activity relationship of PZN and establish the substrate

requirements for the biosynthetic pathway using heterologous expression of PZN analogs in *E. coli*.

RESULTS AND DISCUSSION

Heterologous production of PZN

Although *B. amyloliquefaciens* FZB42 exhibits natural competency (28), the inability to replicate plasmids, coupled with low transformation efficiency of integrative plasmids, necessitated the development of a heterologous system for facile expression and screening of PZN variants. Genomic DNA from the RS32 strain of *B. amyloliquefaciens*, in which the precursor peptide gene (*bamA*) is insertionally disrupted by a spectinomycin resistance cassette (26), was digested and ligated into a DNA vector backbone to generate a fosmid library in *E. coli*. A fosmid bearing the Δ*bamA* PZN biosynthetic gene cluster (Supporting Figure S1) was identified through PCR screening of this library. The Δ*bamA* PZN cluster fosmid was under rhamnose-dependent copy control in *E. coli* (29, 30), while the PZN biosynthetic genes were under control of the native FZB42 promoters. To determine whether the fosmid-borne PZN biosynthetic enzymes were capable of modifying BamA supplied in *trans*, the PZN precursor peptide gene, *bamA*, was cloned into *E. coli* expression vector pBAD24 with an *N*-terminal fusion to maltose-binding protein (MBP) using standard methods (Supporting Table S1). Expression of *bamA* from this construct was under the control of the arabinose-inducible promoter, P_{ara} (31).

Following growth in Luria-Bertani (LB) media supplemented with rhamnose and arabinose, PZN was obtained from the cell surface of the *E. coli* host by non-lytic methanolic extraction. Successful production and export of mature PZN was detected by high-performance liquid chromatography (HPLC) and matrix-assisted laser desorption ionization time-of-flight mass spectrometry (MALDI-MS) analysis (Supporting Figures S1–S2), albeit at ~5% of the 200–300 μg L^{-1} output from the native *B. amyloliquefaciens* producer (27). It is plausible that the lower production level stems from an inefficient usage of *B. amyloliquefaciens* promoters by *E. coli*. *E. coli* cells containing the Δ*bamA* PZN fosmid only produced PZN when complemented with pBAD24-MBP-BamA after induction with rhamnose and arabinose (Supporting Figure S1). As short peptides have poor half-lives in *E. coli* when lacking a fusion partner (32, 33), inclusion of MBP was necessary for detection of PZN produced from plasmid-borne BamA. When the MBP tag was omitted, heterologous production of PZN was below the detection limit within the context of the crude cell surface extract, <20 pg (data not shown).

To provide an internal standard for evaluating the production level of PZN variants, a second fosmid was constructed bearing the PZN biosynthetic gene cluster from *B. amylolique-faciens* FZB42 with the precursor peptide gene (*bamA*) intact. MALDI-MS and HPLC analysis of methanolic surface extracts from *E. coli* bearing this fosmid indicated production and export of mature PZN, even in the absence of the pBAD24-MBP-BamA construct (Supporting Figure S3).

Design and evaluation of BamA mutants

In order to assess the ability of the PZN posttranslational pathway to accept alternate BamA substrates, nine residues in the core region of BamA were targeted for mutagenesis, based on the sequence similarity among the potential PZN producers (Figure 1b, Supporting Figure S4). This subset of the precursor peptide was selected in order to (*i*) include the most-conserved as well as the least-conserved residues; (*ii*) cover both heterocyclized and non-heterocyclized positions; and (*iii*) span the length of the precursor peptide core region. Rather than employ saturation mutagenesis, directed mutant panels were designed at eight of these positions (Supporting Figure S4). Each panel contained conservative and non-

conservative mutations in order to sufficiently explore the available chemical space without generating an unnecessarily large number of mutants. Mutants were prepared by site-directed mutagenesis using primers with rationally chosen degenerate codons at select positions of pBAD24-MBP-BamA (Supporting Table S2). Following mutagenesis, polyclonal plasmid collections were transformed into competent *E. coli* cells bearing the complete PZN gene cluster fosmid. A medium-throughput method was employed to screen clones in groups of 20–40 for production of unnatural PZN analogs. Individual clones were cultured, PZN biosynthetic gene expression was induced with rhamnose and arabinose, and unnatural PZNs were isolated by non-lytic methanolic surface extraction, conditions which preclude isolation of intracellular contaminants. MALDI-MS was used to screen the surface extracts for unnatural PZN variants (Figure 2) and the positive clones were subjected to DNA sequencing (Figure 3). In addition, a selection of plasmids which did not produce a PZN variant were also sequenced in order to identify which precursor peptides were not processed by the posttranslational modifying enzymes (Figure 3). The confirmed DNA sequence and the observed masses enabled deduction of the number and type of posttranslational modifications for each variant (Figure 2). Using data from MALDI-MS analysis, comparison of the peak heights of wild-type PZN (fosmid-borne BamA, *m/z* 1336) and mutant PZN (plasmid-borne mutant BamA, variable mass) yielded a qualitative measure of production levels of the PZN variants (Figure 3). This preliminary assessment of production level enabled determination of which variants most warranted large-scale expression and purification, circumventing the time- and labor-intensive process of doing so with every variant.

Assessment of the 72 mutants of BamA resulted in 29 clones that successfully produced and exported PZN variants within our detection limit (Figure 3). In this *in vivo* production system, a mutant precursor peptide must be successfully accepted as a substrate by multiple steps of the biosynthetic pathway (cyclodehydration, dehydrogenation, and leader peptidolysis), in addition to export, in order to yield a detectable product. Failure of any of these processes to accept an unnatural precursor peptide substrate led to an absence of detectable PZN variant. It is worth noting that such a result would not likely arise from failure at the methylation step of the biosynthetic pathway, as desmethylPZN can be successfully exported by *B. amyloliquefaciens* (27). Of the 29 clones that successfully produced mature PZN variants, 26 had masses consistent with “wild-type-like” modifications: nine azole rings, one azoline ring, leader peptidolysis *N*-terminal to Arg28, and *N*-terminal dimethylation (Figure 1d). Three exceptions, PZN-T40A, -T40I, and -T40V, all produced MALDI-MS data consistent with the presence of one fewer heterocyclizable residue (nine azoles, no azolines) than wild-type PZN, as expected (Figure 3). Three other clones, I34M, T40C, and F41C, each yielded one or more modifications over “wild-type-like” processing, consistent with varying oxidation states at the mutated position (Figures 2a, 4, 5; Supporting Figure S5).

Notably, the mutant *bamA* sequences differed by three nucleotides at most (out of 1394 bp, including MBP tag) and did not contain any rare *E. coli* codons (34). Thus, the expression levels of the MBP-BamA peptides were expectedly comparable (Supporting Figure S6). The lack of detectable PZN variants for some mutants is attributed to the selectivity of the biosynthetic pathway and not to poor expression of the precursor peptide. Ten of the 29 variants which were produced in the greatest quantity (Figure 3), as defined by ion intensity in MALDI-MS relative to that of the PZN internal standard (fosmid-borne *bamA*), were purified by HPLC (Supporting Figures S5, S7–S15). Subsequent tandem, high-resolution Fourier transform mass spectrometry (FTMS) data were consistent with the predicted structures (Figure 4; Supporting Figures S16–S24). Eight of the ten PZN variants that were produced at “high” levels in *E. coli* harbored mutations at positions in PZN that do not receive side chain modifications: Ile34, Ile35, and Phe41 (Figure 3). This production level

trend suggested that the biosynthetic pathway was more tolerant to variation at non-cyclized positions relative to cyclized positions. The two remaining high production variants, PZN-S38C and -T40C (Figure 3), both replace a Ser/Thr with the heterocycle-competent Cys. In each case, the increased production level of the PZN variant was consistent with the increased nucleophilicity of the Cys side chain, which typically enhances the rate of cyclodehydration (35–37).

Substrate tolerance at heterocyclized positions

As the majority of analyzed mutant sequences failed to yield mature PZN variants, the PZN biosynthetic enzymes were less promiscuous *in vivo* than expected based on studies of other TOMMs (17, 35, 37, 38). Cys29 and Cys31, which are invariant throughout the PZN class (Figure 1b) (27), were critical for posttranslational processing of BamA. No mutation at position 29 or 31 led to detectable PZN product formation *in vivo* (Figure 3). Even conservative mutations of Cys to Ser/Thr, or to the azol(in)e mimic Pro (38), failed to produce mature analogs (Figure 3), demonstrating an unusual chemoselectivity for cysteine at these positions (35–37, 39). Multiple attempts to isolate intermediates in the posttranslational cascade through utilization of the MBP tag via amylose affinity purification, coupled with MALDI-MS, were unsuccessful. For both accepted and unaccepted sequences, only the full-length unmodified BamA peptide could be detected in cell lysates. Identical results where obtained even when the arabinose concentration was lowered (serial dilutions to a final concentration of 3 μM) in an attempt to prevent any processed peptide signal from being overwhelemed by newly synthesized BamA (31). This result implies that failure to cyclize a particular residue aborts downstream modification required for maturation and export, and that cyclodehydration is the first committed step in PZN maturation, but this hypothesis will require further confirmation.

In contrast to the invariant Cys at positions 29 and 31 (Figure 3), the PZN biosynthetic pathway tolerated conservative, heterocyclizable mutations at Thr33 and Ser38, but allowed more non-conservative mutations at Thr40 (Figure 3). Consistent with the variation at these positions in other PZN-like precursor peptides (Figure 1b), all other heterocyclizable residues substituted at these three positions resulted in full (“wild-type-like”) maturation of the PZN analog, including cyclodehydration of the substituted residue (Figure 3). The absence of β-nucleophile-containing amino acids at these positions disrupts the contiguous polyheterocyclic structure of PZN. In the case of Thr33 and Ser38, we posit that this disruption prevents the formation of downstream heterocycles, as observed for other TOMM natural products (37, 40). However, the relative promiscuity of the cyclodehydratase was markedly increased at Thr40, as several non-cyclizable, nonpolar residues (Ala, Val, Ile) were tolerated by the biosynthetic pathway, in addition to other heterocyclizable residues (Cys, Ser). The above-described intolerance towards mutations at Cys29 and Cys31, contrasted with the promiscuity at Thr40, suggests *N*- to *C*-terminal processing for PZN, which is the canonical direction of RiPP modification (36, 37, 41). Alternatively, if position 40 is not the last position to be cyclodehydrated, other modifications of PZN certainly do not depend on position 40 being cyclized, unlike the case for positions 29 and 31.

In native PZN, Thr40 is converted to a methyloxazoline (Figure 1d) and is the only heterocycle to evade dehydrogenation (27). Initial MALDI-MS results found that the PZN-T40S and -T40C variants each contained an azoline, presumably at position 40 (Figure 3). Given that thiazolines hydrolyze under mildly acidic conditions much more slowly than the corresponding (methyl)oxazolines (42, 43), we wondered if differential hydrolysis would be useful to rapidly assess the azoline content of natural products (44). Upon exposing native PZN, -T40S, and -T40C to mild aqueous acid, only T40C was hydrolytically stability under the conditions employed (Figure 6). Intriguingly, when the T40C analog was produced in the strain bearing the PZN Δ*bamA* fosmid, the absence of wild-type PZN (*m/z* 1336)

permitted observation of a fully-oxidized variant (deca-azole, *m/z* 1336), which was unreactive towards acid hydrolysis (Figure 6). FTMS/MS analysis confirmed the proposed structures (Figure 4).

Substrate tolerance at non-cyclized positions

As Thr40 could be substituted with noncyclizable residues, the substrate tolerance at naturally occuring noncyclizable residues was evaluated. Ile34 and Phe41 both lie on the *C*-terminal side of a contiguous polyazol(in)e moiety (Figure 1d), prompting the question of whether an additional heterocycle could be formed at these positions. While substitution with cyclizable residues was tolerated at these positions, the side chains did not undergo cyclodehydration (Figure 3), demonstrating that the PZN cyclodehydratase is remarkably regioselective. These structural assignments were supported by MS/MS data on the PZN-F41C and -I34T analogs (Figure 5, Supporting Figure S17). The free thiol of PZN-F41C was clearly susceptible to oxidation, as indicated by the MS-based detected of the sulfinic (R-SO_2H) and sulfonic (R-SO_3H) acid derivatives (Figures 2a, 5). Installation of a stop codon at position 41, however, failed to produce the expected PZN truncation (Figure 3), suggesting that the biosynthetic pathway required the presence of a *C*-terminal flanking residue for a cyclized position, as previously observed for other TOMMs (37, 39).

In the case of PZN-I34T, the newly installed Thr at position 34 could not be definitively proven to remain uncyclized, due to the difficulty of obtaining dissociation between heterocycles during MS/MS (Supporting Figure S17). However, the data were consistent with the presence of five fully-oxidized heterocycles in the *N*-terminal half of the molecule, as seen in wild-type PZN (27). Thus, if the substituted Thr was cyclized, it would require the omission of a normally-installed heterocycle, which seems unlikely. Although the PZN biosynthetic enzymes could tolerate PZN-I34S/T, the pathway was unable to fully process PZN-I34C (Figure 3). It is possible that cyclodehydration of this newly installed Cys resulted in an intermediate that was incompatible with downstream processing. Unfortunately, all attempts to isolate potential biosynthetic intermediates of PZN-I34C resulted in the detection of only the full-length unmodified peptide (data not shown). Indirect support for the incompatibility of cyclization from PZN-I34C comes from variant -I34P, the only other assessed mutant at position 34 that did not produce PZN (Figure 3). As proline is known to mimic azol(in)e heterocycles, the intolerance towards PZN-I34P suggests the inability of the biosynthetic pathway to cope with the lack of conformational flexibility at this position (37, 38).

Among the four residues with unmodified side chains in the core sequence of wild-type BamA, the PZN biosynthetic pathway was least tolerant to mutation at Ile35 and Arg28 (Figure 3). Only conservative mutations were tolerated at Ile35: Ala, Val, and the sterically similar Asn (Figure 3). Many of the substitutions tolerated at Ile34 did not yield detectable mature PZN analogs when probed at Ile35, including Gly, aromatic residues, and polar residues. This trend was consistent with the flanking residue requirements observed with other TOMM cyclodehydratases (37, 39), where the constraints for the residue in the −1 (*N*-terminal) position flanking a heterocycle are stricter than for the residue in the +1 (*C*-terminal) position. In PZN, with its two contiguous polyazol(in)e moieties, Ile35 occupies the −1 position for the *C*-terminal ring system, while Ile34 and Phe41 lie in +1 positions. By extension, Arg28 (N^{α},N^{α}-dimethylarginine in mature PZN) is in the −1 position for the *N*-terminal ring system (Figure 1d). The most conservative mutation possible, R28K, was not tolerated by the PZN biosynthetic pathway, and as such, did not garner further attention (Figure 3). Conceivably, the failure to process the R28K mutant was due to its proximity to the leader peptidase cleavage site, thus inhibiting leader peptide cleavage and export. Numerous attempts to detect intracellular PZN intermediates with intact leader peptides by affinity chromatography were unsuccessful. Post-proteolysis, the methylation state of PZN

should not affect export, as desmethylPZN was successfully exported in a Δ*bamL* strain of *B. amyloliquefaciens* (26, 27).

Pathway tolerance for variations in substrate length

In the continued interest of exploring the substrate tolerance of the PZN biosynthetic pathway, several BamA analogs were constructed to expand the PZN sequence by one residue in the middle of each polyazol(in)e moiety, between the two central Ile residues, and at the *C*-terminus (Supporting Figure S25, Supporting Table S2). Production of PZN variants based on these peptides was assessed as described above. BamA peptides expanded by an internal alanine residue were not processed (Supporting Figure S25). However, expansion of the peptide by a single residue at the *C*-terminus was tolerated in all cases tested, with the exception of proline (Supporting Figure S25). In addition to these expanded substrates, a contracted version of BamA was constructed by deletion of Ser38, potentially reducing the *C*-terminal polyazole system from five heterocycles to four. However, this substrate also eluded processing. Taken together with the failure to process substrates truncated at positions 35 and 41 (Figure 3), these data indicated that one or more of the PZN biosynthetic enzymes have precise length requirements as to the arrangement of heterocyclized residues within the BamA precursor peptide. In this regard, PZN biosynthesis stands in stark contrast to several other characterized TOMM biosynthetic pathways (18, 37, 39).

Production of other PZN-class natural products

Although four other publicly available bacterial genomes encode PZN-like biosynthetic gene clusters (Figure 1), to date, only *Bacillus pumilus* has been shown to produce PZN during laboratory cultivation (27). The amino acid sequences of the core peptides from *B. pumilus* ATCC 7061 and *B. amyloliquefaciens* FZB42 are identical (Figure 1b) (27), rendering it necessary to look to the other potential PZN producers in order to determine if *E. coli* could biosynthesize non-*Bacillus* PZN compounds. As substrate binding is mediated by the leader sequence (38, 45–47), the PZN biosynthetic enzymes from *B. amyloliquefaciens* were unlikely to accept significantly different leader peptides as substrates. Indeed, attempts to heterologously produce the *Clavibacter michiganensis* subsp. *sepedonicus* (Cms) encoded PZN (via pBAD24-MBP-CmsA) using the FZB42 biosynthetic pathway (fosmid-borne) proved unsuccessful. To circumvent the potential failure of leader peptide recognition during *E. coli* heterologous expression, precursor peptide chimeras were generated that consisted of the leader peptide sequence from the native producer (FZB42) and the core peptide sequence from other family members, yielding BamA-CmsA, BamA-CurA, and BamA-BlinA (Cur, *Corynebacterium urealyticum* DSM 7109; Blin, *Brevibacterium linens* BL2, Supporting Figure S26). Similar strategies employing precursor peptide chimeras have been previously used in other RiPP systems to enable the processing of unnatural core peptides (37, 38). Surprisingly, none of the products from the PZN chimeras were detected, although production of the unmodified peptides was verified by MALDI-MS (Supporting Figure S27). The inability to detect PZN-class natural products derived from the chimeric precursor peptides, despite their overall similarity to BamA/PZN, provided further evidence for the extraordinary specificity exhibited by the FZB42 biosynthetic pathway.

To shed further light on the inability of the chimeric peptides to produce PZN variants in *E. coli*, efforts were focused on the PZN cluster from *C. michiganensis*. This cluster bears the highest degree of sequence conservation to FZB42 (aside from *B. pumilus*) among: (*i*) the precursor peptide (51/80; % identity/% similarity), (*ii*) the heterocycle-forming proteins (B: 57/87, C: 41/77, D: 57/76; % identity/% similarity), (*iii*) the other modifying enzymes (E: 16/55, L: 25/60), and (*iv*) the export apparatus (G: 33/71, H: 19/59) (27, 48, 49). In an effort

to render the BamA-CmsA chimera more similar to BamA, two constructs were generated. These included the point mutant BamA-CmsA-S32T and truncation of the *C*-terminal Gly, BamA-CmsA-G42term (Supporting Figure S26). Unexpectedly, these altered BamA-CmsA sequences also failed to produce PZN analogs, indicating that neither of these positions was individually responsible for the failure of BamA-CmsA to be tolerated by the FZB42 pathway. The previously analyzed mutants BamA-I34V and -S38T both yielded mature PZN analogs (Figure 3), indicating that the Val34 or Thr38 residues found in CmsA (Supporting Figure S26) were also not responsible for processing failure. It is not obvious how the two residues in BamA-CmsA flanking Thr38 (*i.e.* Thr37 and Cys39) could pose an obstacle to posttranslational modification. Trp41 also seems an unlikely problem, given that PZN variants at position Phe41 were successfully biosynthesized with a wide variety of amino acid replacements (Figure 3). Taken together, these data indicate that the failure of the PZN pathway to process the BamA-CmsA chimera was not due to a single residue difference in the precursor peptide, but instead a culmination of several amino acid changes.

Antibacterial activity of PZN analogs

Of the 29 PZN variants detected, ten were produced in sufficient quantity (Figure 3) to permit assessment of their antibacterial activity against *B. anthracis* Sterne. These ten analogs, as well as the wild-type BamA sequence, were expressed in conjunction with the PZN Δ*bamA* fosmid, extracted in methanol, and purified by HPLC (Supporting Figures S5, S7–S15), each yielding 3–5 μg of purified PZN analog per 15 cm diameter plate of LB agar. The minimum inhibitory concentrations (MICs) of the purified PZN analogs were then determined by microbroth dilution assay against *B. anthracis* Sterne (Table 1). The activity of heterologously produced wild-type PZN was in good agreement with the published value for PZN from the native host (27). The analogs exhibited a range of antibacterial potencies, although no analogs were observed to have increased potency against *B. anthracis*.

As expected, conservative mutations to the non-cyclized Ile residues (I34V, I34T, I35V) resulted in relatively modest reductions (four- to eight-fold) in antibacterial potency (Table 1). In contrast, PZN-I34M, which lacks a β-methyl side chain substituent, resulted in a 16-fold reduction in potency, indicating that this region of the PZN structure does contribute to the anti-*B. anthracis* activity. Similarly, relatively conservative mutations to the *C*-terminal Phe (F41A, F41L, F41V) also led to modest reductions (two- to eight-fold) in potency. Surprisingly, a conservative mutation at this position, F41Y, abolished the antibacterial activity of PZN (Table 1). The similarly conservative S38C mutation (replaces an oxazole with a thiazole) also resulted in a 16-fold reduction in activity (Table 1). As these moieties are isosteric, the altered activity of the PZN analog must arise from electronic effects.

Analysis of PZN-T40C yielded two analogs differing in heterocycle oxidation at the penultimate position (Figure 4). These species were separable by HPLC (Supporting Figure S11) and tested for anti-*B. anthracis* activity. PZN-T40C(thiazoline) resulted in a four-fold reduction in anti-*B. anthracis* potency, while the presence of the fully oxidized, “deca-azole” T40C(thiazole) resulted in a 16-fold reduction in activity (Table 1). These data indicate that the posttranslational status of position 40 plays an important role in the activity of PZN. These results concur with the previously noted 16-fold loss of activity upon hydrolysis of the Thr40 methyloxazoline in native PZN (Table 1) (27). As expected, none of the oxazoline-containing PZN variants assayed in this study exhibited significant anti-*B. anthracis* activity (MIC <32 μg/mL) when hydrolyzed (Table 1). Analogs lacking a heterocycle at position 40 (PZN-T40A, -T40I, and -T40V; Figure 3) were not isolated in sufficient quantity (>10 μg) to facilitate purification and subsequent determination of antibacterial potency. However, based on the results for hydrolyzed PZN (reinstated Thr at position 40) and T40C, it is likely that these mutations would also severely reduce, if not abolish, activity. In accord with the observation that desmethylPZN had no measurable

activity (27), it is clear that multiple regions of PZN, including both *N*- and *C*-termini, as well as the internal Ile residues and the polyazole(in)e moieties, collectively contribute to the observed anti-*B. anthracis* activity.

In conclusion, we have developed a facile system for the heterologous expression of PZN in *E. coli*, which enabled the production of analogs from variant precursor peptides. Using this system, we have elucidated the scope of substrate tolerance in the PZN biosynthetic pathway and found it to be much less permissive than previously characterized RiPPs. From PZN analogs that were successfully produced, we have also provided significant insight into the structure-activity relationship for the PZN pharmacophore. This heterologous expression system has the potential to be applied to the study of any RiPP natural product by facilitating production of analogs in *E. coli*.

METHODS

Heterologous PZN production

To heterologously produce PZN and analogs, *E. coli* cells containing a fosmid harboring the PZN biosynthetic gene cluster Δ*bamA* (Supporting Methods) were transformed with purified pBAD24-MBP-BamA or a variant thereof. Transformants were selected using Luria-Bertani (LB) agar supplemented with ampicillin (50 μg mL^{-1}) and chloramphenicol (12.5 μg mL^{-1}). Individual colonies were used to inoculate 10 mL cultures of LB broth supplemented with ampicillin (50 μg/mL) and chloramphenicol (12.5 μg mL^{-1}) in test tubes. Cultures were grown on a roller drum at 37 °C to an OD_{600} measurement of 0.6, at which point cells were harvested by centrifugation (4,000 × *g*) and resuspended in 1 mL of the LB supernatant. To induce production of PZN or analogs, 300 μL of cell suspension was spread on a 15 cm plate of LB agar supplemented with ampicillin (50 μg mL^{-1}), chloramphenicol (12.5 μg mL^{-1}), rhamnose (10 mM) to increase copy number of the fosmid (29), and arabinose (10 mM) to induce expression of MBP-BamA from the P_{ara} promoter of pBAD24. These cultures were grown at 30 °C for 40 h. Cells were harvested by resuspension in TE buffer (10 mM Tris, 1 mM EDTA, pH 8.0) and subsequent centrifugation (4,000 × *g*).

PZN extraction

Crude PZN or analogs were obtained by a non-lytic, methanolic cell surface extraction, similar to methods described previously (27). Briefly, cells were resuspended in MeOH (10 mL), agitated by vortex for 45 s, and equilibrated for 15 min at 22 °C. Cells were harvested by centrifugation (4,000 × *g*), and the MeOH supernatant was rotary evaporated to near dryness. The crude extract was resuspended in deionized water and lyophilized to dryness. Dried, crude extracts were resuspended in 500 μL of 80% (v/v) aqueous MeCN for purification by HPLC or in 500 μL MeOH for analysis of crude extract by MALDI-MS.

Screening of mutant panels

To screen BamA mutant panels for production of PZN variants, purified polyclonal plasmid libraries or individual plasmid sequences were used to transform chemically competent *E. coli* cells containing the entire PZN biosynthetic gene cluster (including *bamA*) on a fosmid, as described above. Individual colonies were used to inoculate 10 mL cultures of LB broth supplemented with ampicillin (50 μg mL^{-1}) and chloramphenicol (12.5 μg mL^{-1}) in test tubes. Cultures were grown on a roller drum at 37 °C to an OD_{600} of 0.6, at which point PZN production was induced by addition of rhamnose (10 mM) and arabinose (10 mM) to the liquid cultures. Following induction, cultures were grown with shaking at 30 °C for 24 h. Cells were harvested by centrifugation (4,000 × *g*), washed with TE buffer, and harvested again (8,000 × *g*). PZN variants were extracted analogously to the procedure described above using 1 mL MeOH. Cells were harvested by centrifugation (8,000 × *g*), and the

MeOH supernatant was evaporated in a speed-vac concentrator with minimal heating. Dry, crude extracts were resuspended in 10 μL MeOH for analysis by MALDI-MS. Since the Quikchange™ site-directed mutagenesis method does not guarantee that all possible DNA sequences will be produced due to potential sequence biases, a sufficient number of clones were sequenced from each library to ensure 95% confidence in having detected all generated mutants, as calculated by $0.95 = 1-(1-f)^n$, where f = frequency of the least represented mutants and n = number of clones screened (50).

Reverse phase HPLC purification

Crude PZN or analogs [suspended in 80% (v/v) aqueous MeCN] were reverse phase purified as described previously (27) using a Thermo BETASIL C18 column (250 mm × 10 mm; pore size: 100 Å; particle size: 5 μm) at a flow rate of 4 mL min^{-1}. A gradient of 65–95% MeOH with 0.1% (v/v) formic acid over 32 min was used. The fractions containing PZN or an analog (as monitored by A_{266} and later verified by MALDI-MS) were collected into 20 mL borosilicate vials and the solvent was removed *in vacuo*. Purified PZN analogs were quantified by A_{260} in DMSO solution.

Mass spectrometry

MALDI-MS analysis used a Bruker Daltonics UltrafleXtreme MALDI-TOF/TOF instrument operating in reflector/positive mode using sinapic acid as the matrix. LC-MS analysis used an Agilent 1200 HPLC system coupled to a G1956B quadrupole mass spectrometer with an electrospray ionization (ESI) source. LC used a 2.1 mm × 150 mm Grace Vydac Denali C_{18} column (120 Å, 5 μm) with a gradient of 65–95% MeOH with 0.1% (v/v) formic acid over 25 min, with the analytes eluted directly into the MS.

HPLC-purified samples for high-resolution and tandem mass spectrometry were resuspended in 12 μL of 80% (v/v) MeCN with 1% (v/v) formic acid. An Advion Nanomate 100 directly infused the sample to a ThermoFisher Scientific LTQ-FT hybrid linear ion trap, operating at 11 T (calibrated weekly). The FTMS was operated using the following parameters: minimum target signal counts, 5000; resolution, 100,000; *m/z* range detected, dependent on target *m/z*; isolation width (MS/MS), 4–5 *m/z*; normalized collision energy (MS/MS), 35; activation *q* value (MS/MS), 0.4; activation time (MS/MS), 30 ms.

Antibacterial activity assay

Determination of MIC values for PZN analogs was performed as described previously (27) for *B. anthracis* Sterne with the only modification being that PZN analogs were added from DMSO solutions to a maximum final concentration of 32 μg/mL in bacterial cultures. Hydrolyzed samples were prepared by incubation of purified PZN analogs (suspended in MeOH) with 0.2% (w/v) HCl for 4 h at 23 °C, followed by removal of solvent in a speed-vac concentrator and subsequent resuspension in DMSO.

Supplementary Material

Refer to Web version on PubMed Central for supplementary material.

Acknowledgments

We are grateful to W. Metcalf and J. Cronan for the generous gifts of fosmid generation reagents and pBAD24, respectively. We also thank members of the Mitchell lab for the critical review of this manuscript. This work was supported in part by the US National Institutes of Health (NIH, 1R01 GM097142 to D.A.M.), the NIH Director's New Innovator Award Program (DP2 OD008463 to D.A.M.), the Robert C. and Carolyn J. Springborn Endowment (to C.D.D.), and the Cell & Molecular Biology Training Grant (T32 GM007283 to K.J.M.). The Bruker

UltrafleXtreme MALDI TOF/TOF mass spectrometer was purchased in part with a grant from the National Center for Research Resources, NIH (S10 RR027109 A).

References

1. Fischbach MA, Walsh CT. Antibiotics for emerging pathogens. Science. 2009; 325:1089–1093. [PubMed: 19713519]
2. Newman DJ, Cragg GM. Natural Products As Sources of New Drugs over the 30 Years from 1981 to 2010. J Nat Prod. 2012; 75:311–335. [PubMed: 22316239]
3. Challis GL. Genome mining for novel natural product discovery. J Med Chem. 2008; 51:2618–2628. [PubMed: 18393407]
4. Kapur S, Chen AY, Cane DE, Khosla C. Molecular recognition between ketosynthase and acyl carrier protein domains of the 6-deoxyerythronolide B synthase. Proc Natl Acad Sci U S A. 2010; 107:22066–22071. [PubMed: 21127271]
5. Kapur S, Lowry B, Yuzawa S, Kenthirapalan S, Chen AY, Cane DE, Khosla C. Reprogramming a module of the 6-deoxyerythronolide B synthase for iterative chain elongation. Proc Natl Acad Sci U S A. 2012; 109:4110–4115. [PubMed: 22371562]
6. Liu T, Chiang YM, Somoza AD, Oakley BR, Wang CC. Engineering of an “unnatural” natural product by swapping polyketide synthase domains in Aspergillus nidulans. J Am Chem Soc. 2011; 133:13314–13316. [PubMed: 21815681]
7. Hughes AJ, Keatinge-Clay A. Enzymatic extender unit generation for in vitro polyketide synthase reactions: structural and functional showcasing of Streptomyces coelicolor MatB. Chem Biol. 2011; 18:165–176. [PubMed: 21338915]
8. Arnison PG, Bibb MJ, Bierbaum G, Bowers AA, Bugni TS, Bulaj G, Camarero JA, Campopiano DJ, Challis GL, Clardy J, Cotter PD, Craik DJ, Dawson M, Dittmann E, Donadio S, Dorrestein PC, Entian KD, Fischbach MA, Garavelli JS, Goransson U, Gruber CW, Haft DH, Hemscheidt TK, Hertweck C, Hill C, Horswill AR, Jaspars M, Kelly WL, Klinman JP, Kuipers OP, Link AJ, Liu W, Marahiel MA, Mitchell DA, Moll GN, Moore BS, Muller R, Nair SK, Nes IF, Norris GE, Olivera BM, Onaka H, Patchett ML, Piel J, Reaney MJT, Rebuffat S, Ross RP, Sahl HG, Schmidt EW, Selsted ME, Severinov K, Shen B, Sivonen K, Smith L, Stein T, Sussmuth RD, Tagg JR, Tang GL, Truman AW, Vederas JC, Walsh CT, Walton JD, Wenzel SC, Willey JM, van der Donk WA. Ribosomally synthesized and post-translationally modified peptide natural products: overview and recommendations for a universal nomenclature. Nat Prod Rep. 2013; 30:108–160. [PubMed: 23165928]
9. Piper C, Hill C, Cotter PD, Ross RP. Bioengineering of a Nisin A-producing Lactococcus lactis to create isogenic strains producing the natural variants Nisin F, Q and Z. Microb Biotechnol. 2011; 4:375–382. [PubMed: 21375711]
10. Molloy EM, Field D, Connor PM, Cotter PD, Hill C, Ross RP. Saturation mutagenesis of lysine 12 leads to the identification of derivatives of nisin a with enhanced antimicrobial activity. PloS one. 2013; 8:e58530. [PubMed: 23505531]
11. Molloy EM, Ross RP, Hill C. ‘Bac’ to the future: bioengineering lantibiotics for designer purposes. Biochem Soc Trans. 2012; 40:1492–1497. [PubMed: 23176504]
12. Cotter PD, Deegan LH, Lawton EM, Draper LA, O’Connor PM, Hill C, Ross RP. Complete alanine scanning of the two-component lantibiotic lacticin 3147: generating a blueprint for rational drug design. Mol Microbiol. 2006; 62:735–747. [PubMed: 17076667]
13. Field D, Molloy EM, Iancu C, Draper LA, O’Connor PM, Cotter PD, Hill C, Ross RP. Saturation mutagenesis of selected residues of the alpha-peptide of the lantibiotic lacticin 3147 yields a derivative with enhanced antimicrobial activity. Microb Biotechnol. 2013
14. Appleyard AN, Choi S, Read DM, Lightfoot A, Boakes S, Hoffmann A, Chopra I, Bierbaum G, Rudd BA, Dawson MJ, Cortes J. Dissecting structural and functional diversity of the lantibiotic mersacidin. Chem Biol. 2009; 16:490–498. [PubMed: 19477413]
15. Caetano T, Krawczyk JM, Mosker E, Sussmuth RD, Mendo S. Heterologous expression, biosynthesis, and mutagenesis of type II lantibiotics from Bacillus licheniformis in Escherichia coli. Chem Biol. 2011; 18:90–100. [PubMed: 21276942]

16. Boakes S, Ayala T, Herman M, Appleyard AN, Dawson MJ, Cortes J. Generation of an actagardine A variant library through saturation mutagenesis. Appl Microbiol Biotechnol. 2012; 95:1509–1517. [PubMed: 22526797]
17. Bowers AA, Acker MG, Koglin A, Walsh CT. Manipulation of thiocillin variants by prepeptide gene replacement: structure, conformation, and activity of heterocycle substitution mutants. J Am Chem Soc. 2010; 132:7519–7527. [PubMed: 20455532]
18. Bowers AA, Acker MG, Young TS, Walsh CT. Generation of thiocillin ring size variants by prepeptide gene replacement and in vivo processing by Bacillus cereus. J Am Chem Soc. 2012; 134:10313–10316. [PubMed: 22686940]
19. Li C, Zhang F, Kelly WL. Heterologous production of thiostrepton A and biosynthetic engineering of thiostrepton analogs. Mol Biosyst. 2011; 7:82–90. [PubMed: 21107477]
20. Li C, Zhang F, Kelly WL. Mutagenesis of the thiostrepton precursor peptide at Thr7 impacts both biosynthesis and function. Chem Commun. 2012; 48:558–560.
21. Young TS, Dorrestein PC, Walsh CT. Codon randomization for rapid exploration of chemical space in thiopeptide antibiotic variants. Chem Biol. 2012; 19:1600–1610. [PubMed: 23261603]
22. Tianero MD, Donia MS, Young TS, Schultz PG, Schmidt EW. Ribosomal route to small-molecule diversity. J Am Chem Soc. 2012; 134:418–425. [PubMed: 22107593]
23. Pan SJ, Link AJ. Sequence diversity in the lasso peptide framework: discovery of functional microcin J25 variants with multiple amino acid substitutions. J Am Chem Soc. 2011; 133:5016–5023. [PubMed: 21391585]
24. Lee SW, Mitchell DA, Markley AL, Hensler ME, Gonzalez D, Wohlrab A, Dorrestein PC, Nizet V, Dixon JE. Discovery of a widely distributed toxin biosynthetic gene cluster. Proc Natl Acad Sci U S A. 2008; 105:5879–5884. [PubMed: 18375757]
25. Dunbar KL, Melby JO, Mitchell DA. YcaO domains use ATP to activate amide backbones during peptide cyclodehydrations. Nat Chem Biol. 2012; 8:569–575. [PubMed: 22522320]
26. Scholz R, Molohon KJ, Nachtigall J, Vater J, Markley AL, Sussmuth RD, Mitchell DA, Borriss R. Plantazolicin, a novel microcin B17/streptolysin S-like natural product from Bacillus amyloliquefaciens FZB42. J Bacteriol. 2011; 193:215–224. [PubMed: 20971906]
27. Molohon KJ, Melby JO, Lee J, Evans BS, Dunbar KL, Bumpus SB, Kelleher NL, Mitchell DA. Structure determination and interception of biosynthetic intermediates for the plantazolicin class of highly discriminating antibiotics. ACS Chem Biol. 2011; 6:1307–1313. [PubMed: 21950656]
28. Idris EE, Iglesias DJ, Talon M, Borriss R. Tryptophan-dependent production of indole-3-acetic acid (IAA) affects level of plant growth promotion by Bacillus amyloliquefaciens FZB42. Mol Plant Microbe Interact. 2007; 20:619–626. [PubMed: 17555270]
29. Eliot AC, Griffin BM, Thomas PM, Johannes TW, Kelleher NL, Zhao H, Metcalf WW. Cloning, expression, and biochemical characterization of Streptomyces rubellomurinus genes required for biosynthesis of antimalarial compound FR900098. Chem Biol. 2008; 15:765–770. [PubMed: 18721747]
30. Bates PF, Swift RA. Double cos site vectors: simplified cosmid cloning. Gene. 1983; 26:137–146. [PubMed: 6323255]
31. Guzman LM, Belin D, Carson MJ, Beckwith J. Tight regulation, modulation, and high-level expression by vectors containing the arabinose PBAD promoter. J Bacteriol. 1995; 177:4121–4130. [PubMed: 7608087]
32. Kuliopulos A, Walsh CT. Production, purification, and cleavage of tandem repeats of recombinant peptides. J Am Chem Soc. 1994; 116:4599–4607.
33. Kapust RB, Routzahn KM, Waugh DS. Processive degradation of nascent polypeptides, triggered by tandem AGA codons, limits the accumulation of recombinant tobacco etch virus protease in Escherichia coli BL21(DE3). Protein Expr Purif. 2002; 24:61–70. [PubMed: 11812224]
34. Bouallag N, Gaillard C, Marechal V, Strauss F. Expression of Epstein-Barr virus EBNA1 protein in Escherichia coli: purification under nondenaturing conditions and use in DNA-binding studies. Protein Expr Purif. 2009; 67:35–40. [PubMed: 19393319]
35. Belshaw PJ, Roy RS, Kelleher NL, Walsh CT. Kinetics and regioselectivity of peptide-to-heterocycle conversions by microcin B17 synthetase. Chem Biol. 1998; 5:373–384. [PubMed: 9662507]

36. Kelleher NL, Hendrickson CL, Walsh CT. Posttranslational heterocyclization of cysteine and serine residues in the antibiotic microcin B17: distributivity and directionality. Biochemistry. 1999; 38:15623–15630. [PubMed: 10569947]
37. Melby JO, Dunbar KL, Trinh NQ, Mitchell DA. Selectivity, directionality, and promiscuity in peptide processing from a Bacillus sp. Al Hakam cyclodehydratase. J Am Chem Soc. 2012; 134:5309–5316. [PubMed: 22401305]
38. Mitchell DA, Lee SW, Pence MA, Markley AL, Limm JD, Nizet V, Dixon JE. Structural and functional dissection of the heterocyclic peptide cytotoxin streptolysin S. J Biol Chem. 2009; 284:13004–13012. [PubMed: 19286651]
39. Sinha Roy R, Belshaw PJ, Walsh CT. Mutational analysis of posttranslational heterocycle biosynthesis in the gyrase inhibitor microcin B17: distance dependence from propeptide and tolerance for substitution in a GSCG cyclizable sequence. Biochemistry. 1998; 37:4125–4136. [PubMed: 9521734]
40. Roy RS, Allen O, Walsh CT. Expressed protein ligation to probe regiospecificity of heterocyclization in the peptide antibiotic microcin B17. Chem Biol. 1999; 6:789–799. [PubMed: 10574779]
41. Lee MV, Ihnken LA, You YO, McClerren AL, van der Donk WA, Kelleher NL. Distributive and directional behavior of lantibiotic synthetases revealed by high-resolution tandem mass spectrometry. J Am Chem Soc. 2009; 131:12258–12264. [PubMed: 19663480]
42. Martin RB, Parcell A. Hydrolysis of 2-methyl-delta-oxazoline - an intramolecular O-N-acetyl transfer reaction. J Am Chem Soc. 1961; 83:4835–4838.
43. Martin RB, Hedrick RI, Parcell A. Thiazoline + oxazoline hydrolyses + sulfur-nitrogen + oxygen-nitrogen acyl transfer reactions. J Org Chem. 1964; 29:3197–3206.
44. Dunbar KL, Mitchell DA. Insights into the mechanism of peptide cyclodehydrations achieved through the chemoenzymatic generation of amide derivatives. J Am Chem Soc. 2013; 135:8692–8701. [PubMed: 23721104]
45. Roy RS, Kim S, Baleja JD, Walsh CT. Role of the microcin B17 propeptide in substrate recognition: solution structure and mutational analysis of McbA1-26. Chem Biol. 1998; 5:217–228. [PubMed: 9545435]
46. Madison LL, Vivas EI, Li YM, Walsh CT, Kolter R. The leader peptide is essential for the post-translational modification of the DNA-gyrase inhibitor microcin B17. Mol Microbiol. 1997; 23:161–168. [PubMed: 9004229]
47. Oman TJ, van der Donk WA. Follow the leader: the use of leader peptides to guide natural product biosynthesis. Nat Chem Biol. 2010; 6:9–18. [PubMed: 20016494]
48. Bentley SD, Corton C, Brown SE, Barron A, Clark L, Doggett J, Harris B, Ormond D, Quail MA, May G, Francis D, Knudson D, Parkhill J, Ishimaru CA. Genome of the actinomycete plant pathogen Clavibacter michiganensis subsp. sepedonicus suggests recent niche adaptation. J Bacteriol. 2008; 190:2150–2160. [PubMed: 18192393]
49. Chen XH, Koumoutsi A, Scholz R, Eisenreich A, Schneider K, Heinemeyer I, Morgenstern B, Voss B, Hess WR, Reva O, Junge H, Voigt B, Jungblut PR, Vater J, Sussmuth R, Liesegang H, Strittmatter A, Gottschalk G, Borriss R. Comparative analysis of the complete genome sequence of the plant growth-promoting bacterium Bacillus amyloliquefaciens FZB42. Nat Biotechnol. 2007; 25:1007–1014. [PubMed: 17704766]
50. Jeltsch A, Lanio T. Site-directed mutagenesis by polymerase chain reaction. Methods Mol Biol. 2002; 182:85–94. [PubMed: 11768980]

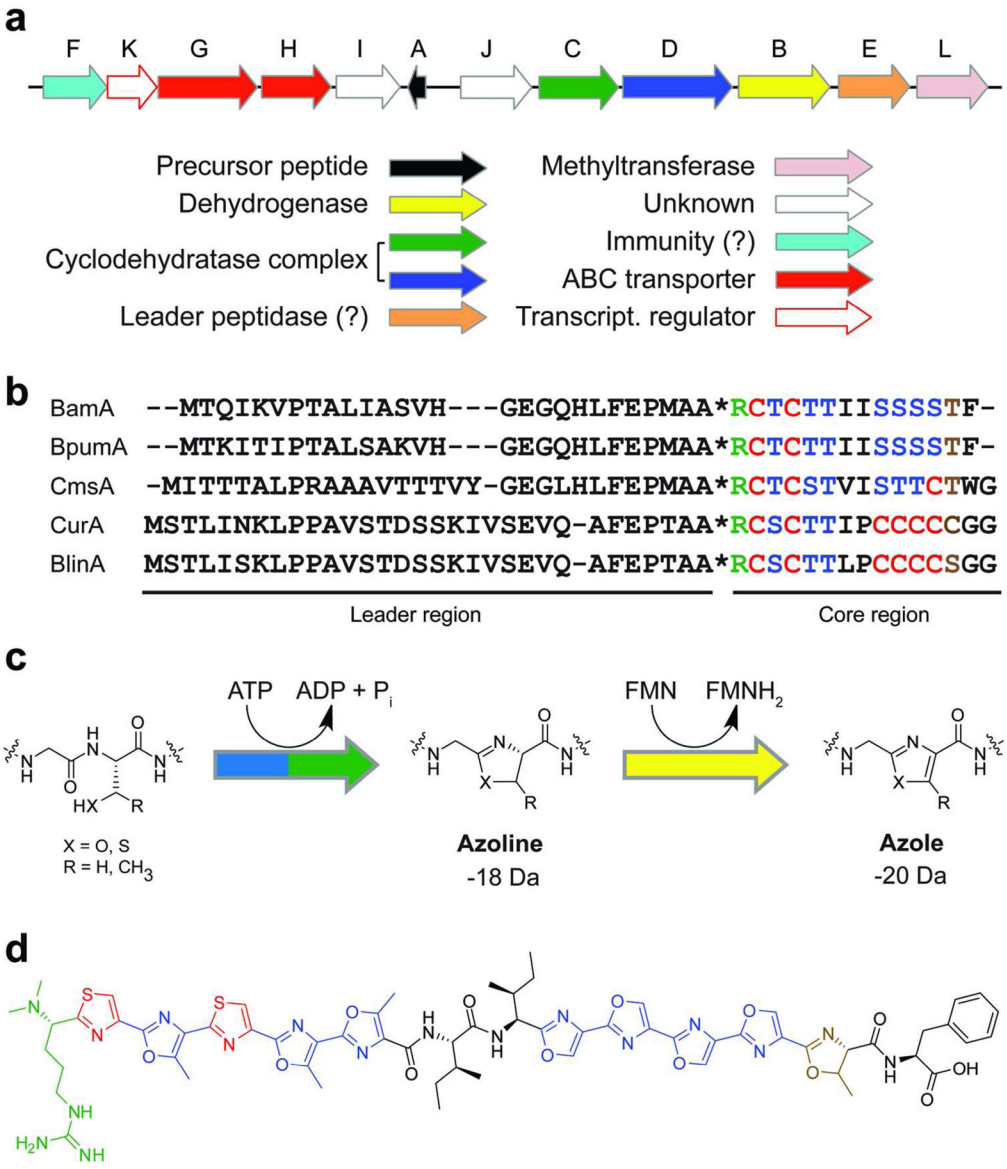

Figure 1.

Genetics and enzymology of PZN biosynthesis. (a) The 10 kb PZN biosynthetic gene cluster from *Bacillus amyloliquefaciens* FZB42. (b) The precursor peptides for PZN and potential analogs from other species exhibit remarkable similarity. Bam, *B. amyloliquefaciens* FZB42; Bpum, *B. pumilus* ATCC 7061; Cms, *Clavibacter michiganensis* subsp. *sepedonicus*; Cur, *Corynebacterium urealyticum* DSM 7109; Blin, *Brevibacterium linens* BL2. Color-coding (predicted for Cms, Cur, and Blin): green, N^{α},N^{α}-dimethylarginine; red, thiazoles; blue (methyl)oxazoles; brown, methyloxazoline; *, peptidase cleavage site. (c) Posttranslational modification of cysteine, serine, and threonine residues in TOMM biosynthesis proceeds by cyclodehydration (mass loss of 18 Da) and subsequent oxidation (additional mass loss of 2 Da). (d) The chemical structure of PZN. Color-coding is identical to panel b.

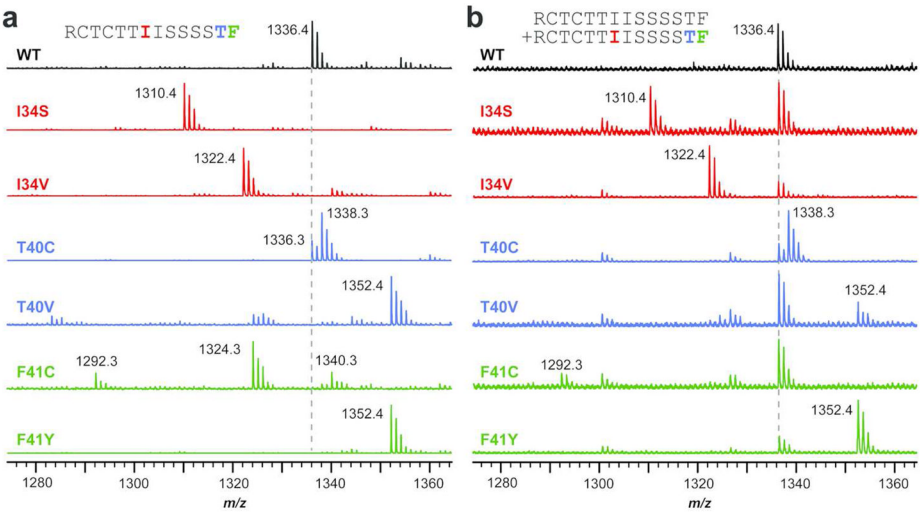

Figure 2.

Representative MALDI mass spectra of PZN analogs. (a) Methanolic surface extracts from *E. coli* containing the PZN cluster Δ*bamA* fosmid plus BamA mutant plasmids. Color-coding: red, I34X mutants; blue, T40X mutants; green, F41X mutants. As indicated by the peak labels and the lack of *m/z* 1336 in each sample, production of PZN variants is only possible from plasmid-borne *mbp-bamA*. The *m/z* 1336 signal in the T40C spectrum corresponds to a variant containing a thiazole at position 40 (confirmation of structure given in Supporting Figure S20). The peaks at *m/z* 1324 and 1340 in the F41C spectrum correspond to oxidized *C*-terminal Cys (R-SO_xH, x = 2–3). Other labeled peaks correspond to PZN variants with wild-type-like modifications. (b) Same as panel a, but with the full PZN cluster fosmid plus BamA mutant plasmids. Wild-type PZN (*m/z* 1336) appears in every sample.

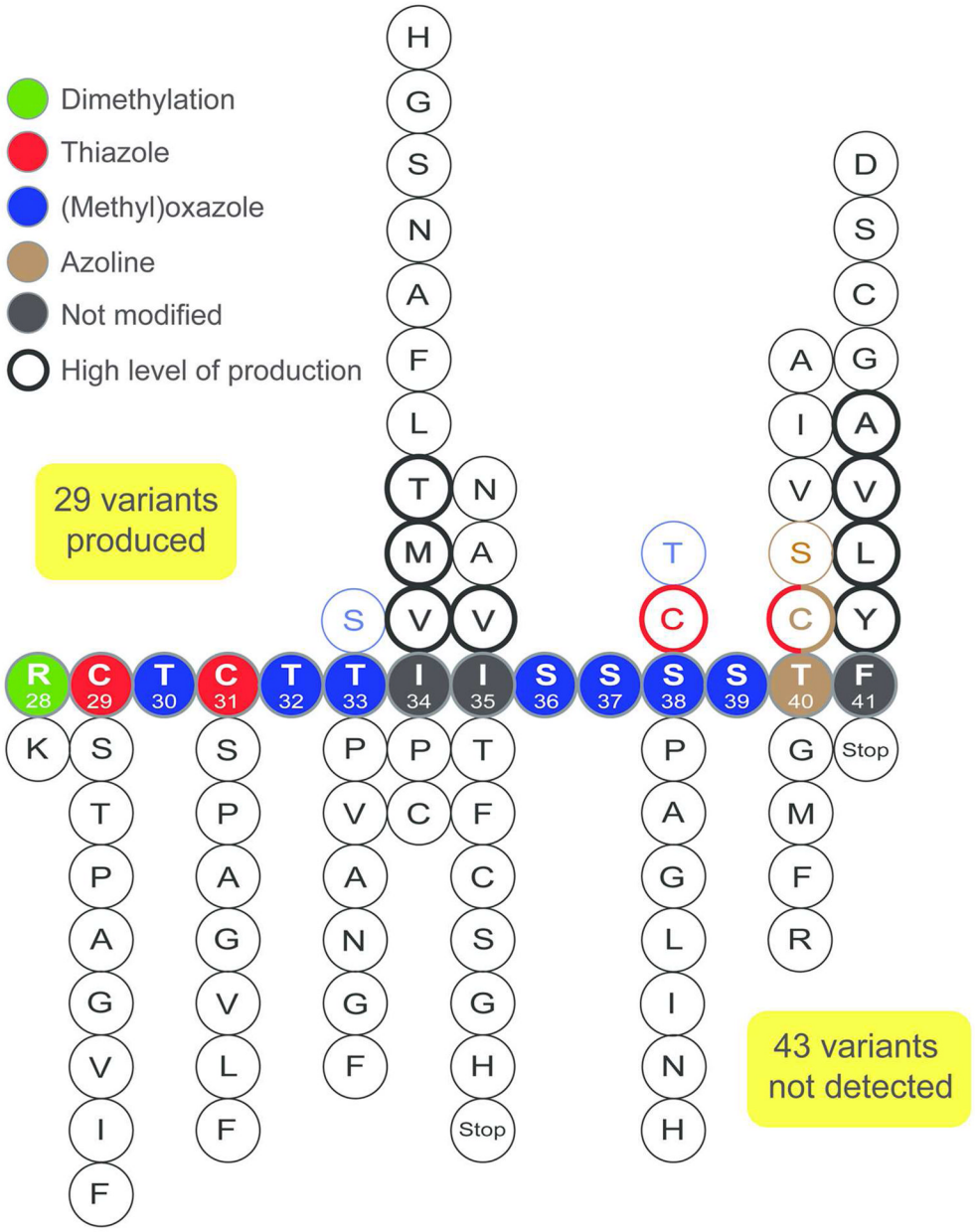

Figure 3.

Summary of PZN variant production. PZN variants were heterologously expressed in *E. coli* prior to methanolic surface extraction and MALDI-MS analysis. Using this method, 29 point mutants of BamA were successfully converted to PZN variants (listed above core sequence), while 43 were not detected (listed below core sequence). Colored outlines indicate modifications to the altered residue as specified in the figure legend. Of the 29 analogs produced above the limit of detection (>20 pg in crude surface extracts), 10 were produced at levels greater than or equal to that of wild-type PZN (bold outlines), as assessed by relative peak heights during MALDI-MS analysis. The T40C variant produced two analogs, one with a thiazole at position 40 and the other with a thiazoline.

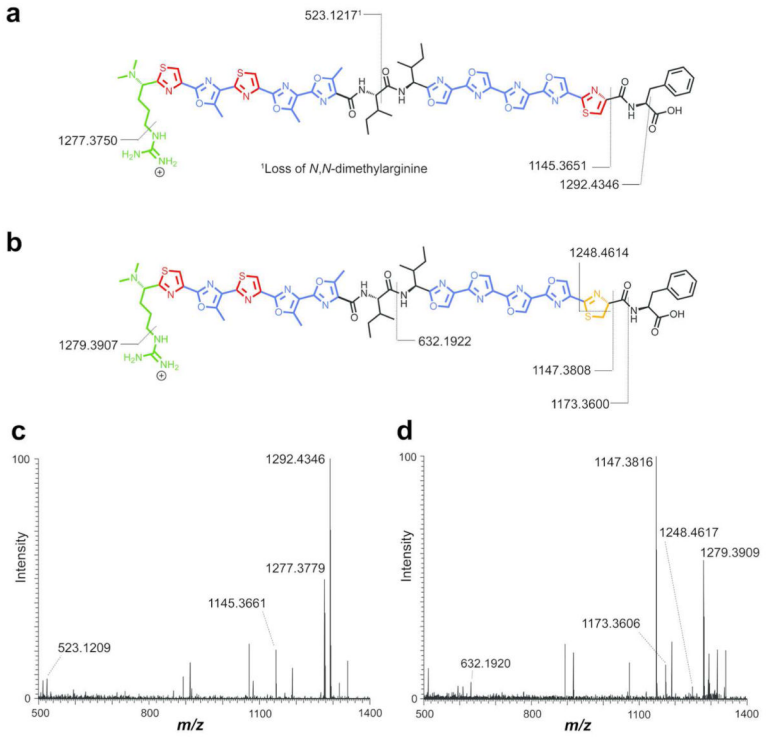

Figure 4.

High resolution, Fourier transform mass spectrometric (FTMS) analysis of PZN-T40C variants. (a) Structure, predicted fragments, and the calculated monoisotopic masses for PZN-T40C (deca-azole variant). One of the fragments was derived from multiple bond cleavages, denoted by the superscript. (b) Same as panel a, but for PZN-T40C (thiazoline variant). The thiazoline moiety is shown in orange. (c) Collision-induced dissociation of PZN-T40C (deca-azole variant, $C_{62}H_{65}N_{17}O_{12}S_3$, *calc. m/z* 1336.4239; *expt. m/z* 1336.4243, error 0.2 ppm) was consistent with the predicted structure. (d) Collision-induced dissociation of PZN-T40C (thiazoline variant, $C_{62}H_{67}N_{17}O_{12}S_3$, *calc. m/z* 1338.4395; *expt. m/z* 1338.4395, error 0.0 ppm) was consistent with the predicted structure, including localization of the thiazoline to position 40.

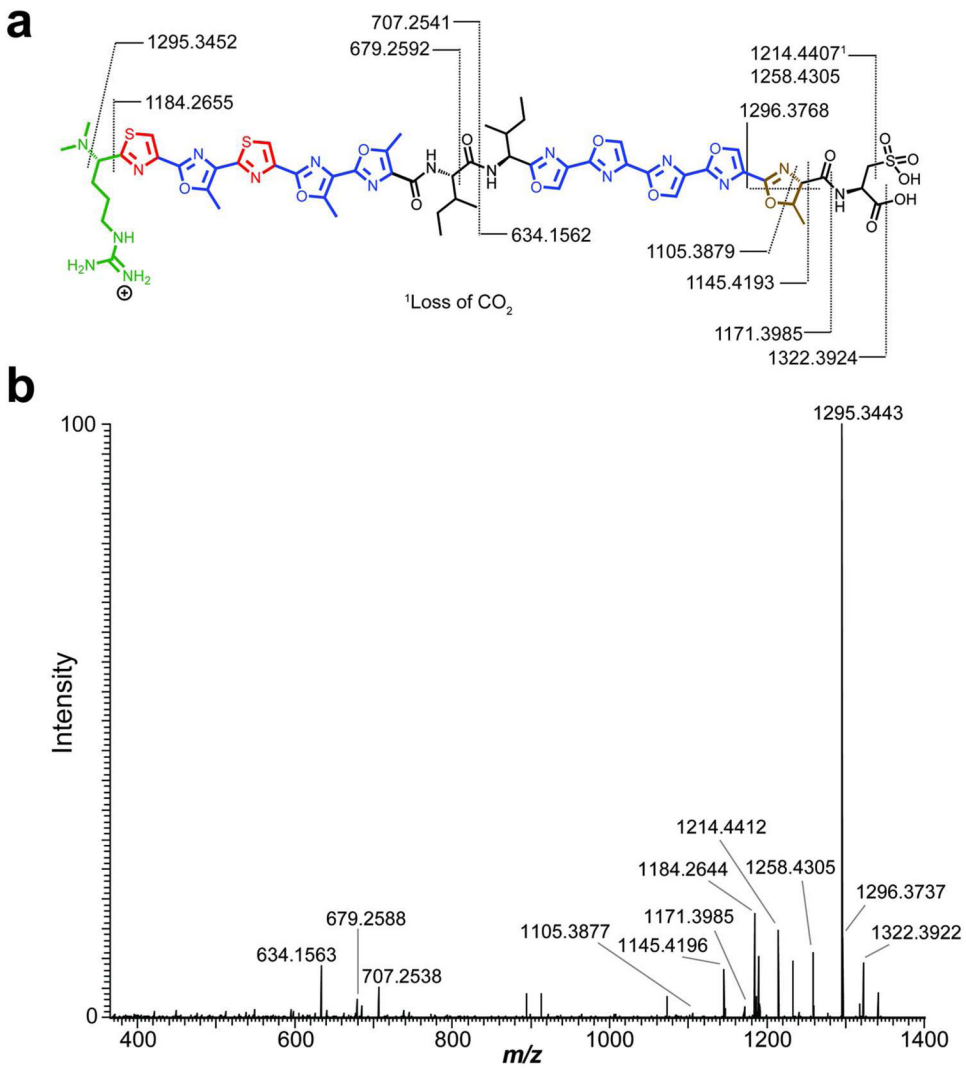

Figure 5.

Fourier transform mass spectrometric (FTMS) analysis of PZN-F41C. (a) Structure, predicted fragments, and calculated monoisotopic masses for a sulfonic acid derivative of PZN-F41C. One of the fragments was derived from multiple bond cleavages, denoted by the superscript. (b) Collision-induced dissociation of PZN-F41C (sulfonic acid derivative, $C_{57}H_{65}N_{17}O_{16}S_3$, *calc. m/z* 1340.4036; *expt. m/z* 1340.4035, error 0.1 ppm) permitted localization of the sulfonic acid moiety to position 41.

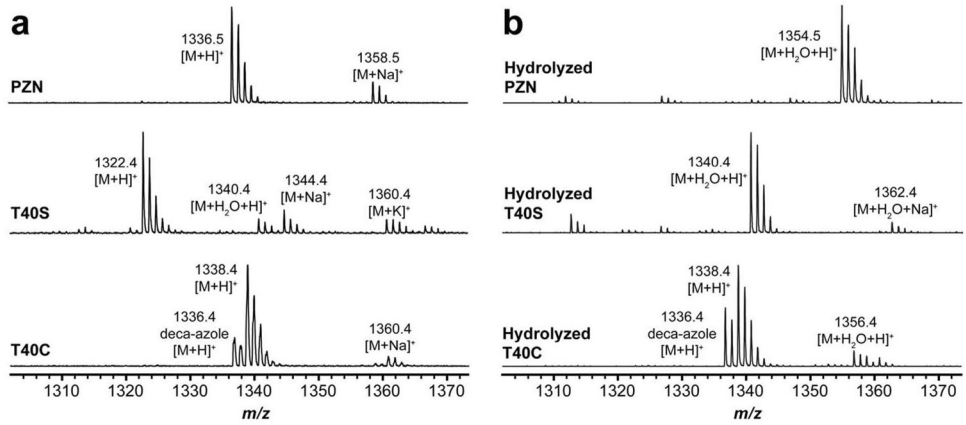

Figure 6.

Hydrolytic stability of PZN analogs varied at Thr40. In naturally occurring PZN, Thr40 exists as a methyloxazoline. (a) MALDI-MS spectra from methanolic surface extracts of *E. coli* engineered to produced native PZN, -T40S, and -T40C. (b) Same as panel a, after treatment with 0.2% HCl for 4 h at 23 °C to induce hydrolysis. Under these conditions, the (methyl)oxazolines were virtually quantitatively hydrolyzed while the T40C thiazoline was minimally hydrolyzed. The deca-azole variant contains a thiazole at position 40, which was unreactive towards hydrolysis.

Table 1

Antibacterial activity of PZN analogs against *B. anthracis* Sterne.

Variant	MIC[a] (μg mL^{-1}) heterocycle at 40	MIC (μg mL^{-1}) Thr at 40
PZN	2	32[b]
I34M	32	>32
I34T	8	>32
I34V	8	>32
I35V	16	32
S38C	32	>32
T40C (thiazoline)	8	N.D.[c]
T40C (thiazole)	32	N/A[d]
F41A	8	32
F41L	4	>32
F41V	16	32
F41Y	>32	>32

[a] MIC = minimum inhibitory concentration.

[b] Ref. (27).

[c] N.D. = not determined.

[d] N/A = not applicable.